Inorganica Chimica Acta, 116 (1986) 85–93

Cone Packing Model – a Geometrical Approach to Coordination and Organometallic Chemistry of Lanthanides and Actinides

LI XING-FU*, FENG XI-ZHANG, XU YING-TING, WANG HAI-TUNG, SHI JIE, LIU LI

Application Department, The Institute of High Energy Physics, Academia Sinica, P.O. Box 2732, Beijing, China

and SUN PENG-NIAN

Department of Biology, The University of Science and Technology of China, Hefei, China

(Received September 27, 1985)

Abstract

By projection of the ligands to a unit sphere centred at the metal ion, steric effects, both local and overall, can be studied quantitatively in terms of solid angle factor (*SAF*), fan angle (*FA*), coordination vector, gap and hole. The packing saturation rule and the packing centre rule have been determined by treatment of more than 400 structures of lanthanide and actinide coordination and organometallic compounds. A ligand packing model was thus adopted with cones joined at the same apex.

'Coordination Saturation' in f-block chemistry was clarified to be saturation in coordination space, implying an equilibrium between bonding and steric effects. Molecular structures could be simulated on the basis of a uniform packing principle. The cone packing model has been applied to inorganic preparation, synergistic extraction and structure prediction. These predictions have been clearly substantiated experimentally, and the results are reported.

A dynamic packing model was also suggested to study the reaction pathways by simulating the relative positions during the reaction process and the size and shape of holes, which correspond to the reaction areas in the coordination sphere. Lewis base association and dissociation, and the metal–carbon bond thermolysis of structural pattern MCp_3L were explained as examples.

Introduction

Two essential interactions exist in coordination and organometallic chemistry. The first is the bondings between the metal ion and the ligands and the second is steric interactions among the ligands due to their geometrical factors such as size and shape. It is quite surprising that whereas most interest has been concentrated on the study of bonding, very little attention has been given to the study of steric effects apart from some empirical and qualitative explanations.

Tolman [1] made the first attempt to quantify steric effects by using the cone angle to describe phosphine ligands and the related physical, chemical and catalytic properties of their complexes. His work has been extended to the concept of ligand profiles [2]. Recently, the use of the solid angle [3] to describe steric effects was introduced by several authors at about the same time [4–7].

Energy change of a complex in comparison to its component ligands is mainly due to bond energy E_{M-L} and ligand–ligand non-bonding interactions E_{L-L}, shown in Fig. 1. To obtain a distinct steric effect, compounds with weak metal–ligand bond interactions were suggested for study so that less interference from orbital interaction would be added to the steric effect. On this point, while Tolman's work was concentrated in the d-transition metal compounds, for which both bonding and steric effects are strong and interfere with each other, our research is directed toward compounds with more ionic bonding, which is characteristically non-directional and non-saturated. Molecular structure might be predominantly dependent on the steric factors. Orbital interactions will not overshadow the steric effects.

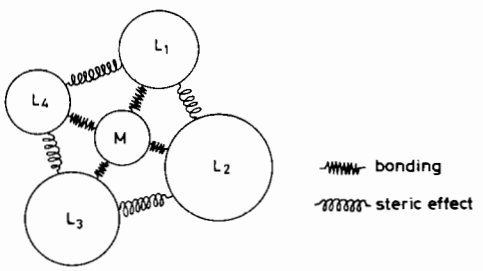

Fig. 1. Packing model of ideal ionic coordination and organometallic compounds.

*Author to whom correspondence should be addressed.

0020-1693/86/$3.50

The chemistry of the s-block elements, *i.e.*, alkali and alkali earth, might be the most appropriate for studying steric effect. However, the structures collected so far are not sufficient for a comprehensive study. In spite of the fact that coordination and organometallic compounds of the f-block are less ionic than those of the s-block, they have obviously different properties in comparison to their d-block analogues, such as:

(a) their coordination can be interpreted as referring to saturation with respect to either coordination number or coordination space;

(b) unexplained disproportionation often occurs, such as 'UCp_2Cl_2' → $UCp_3Cl + UCpCl_3thf_2$;

(c) non-integral-ligand complexes are not uncommon, e.g. $UCl_4dma_{2.5}$, $Th(NO_3)_4$ 2.67tmpo, $LnCl_3$-$dma_{3.5}$, $Ln(NO_3)_3$ 0.67dcc;

(d) there are irregularities in bond length of lanthanide and actinide compounds.

All these phenomena imply a rather high steric effect and some hint of a packing problem. Recently, rapid development in these fields has provided hundreds of molecular structures which make an exhaustive study possible.

In the present paper, we report our preliminary results in the quantitative study of steric effects with lanthanide and actinide coordination and organometallic chemistry as a test field.

Bond distances between the metal ion and coordinating atoms are normally in the range of 2–3 Å, with little overlap. We have adopted a unit sphere with the metal ion as the sphere centre; then we projected the ligands centripetally in the sequence of the first and the second order towards the spherical surface. Geometrically the solid angle factor (*SAF*) is the ratio of the ligand area to 4π. The fan angle (*FA*) is one half of the subtended angle of the area in a certain direction. In fact, the fan angle, when considered in the second order, is the same as Tolman's cone angle. The third concept introduced here is a unit vector $\vec{r}$, directed from the metal towards the centre of the coordinating atom. *SAF*, *FA* and $\vec{r}$ represent the ligand size, shape, and position, respectively (Fig. 2). For multidentate ligands, overlap of van der Waals spheres between their coordinating atoms must be corrected. For example, bidentate nitrate in the structure of $Ce(NO_3)_6^{3-}$ has *SAF* of 0.0852 for each of its coordinating oxygen atom whereas the whole nitrate ligand has an *SAF* of 0.157 with the correction of −0.013 for their overlapping. The nitrate ligand has two fan angles, 59.5° along and 33.9° across the ligand plane. The second order steric effect is related to the next layer of noncoordinated atoms of ligands at a projected distance of between 3.5 to 4.5 Å from the metal ion.

The symbol G was used to describe the gap between the projectional areas of two ligands. It is

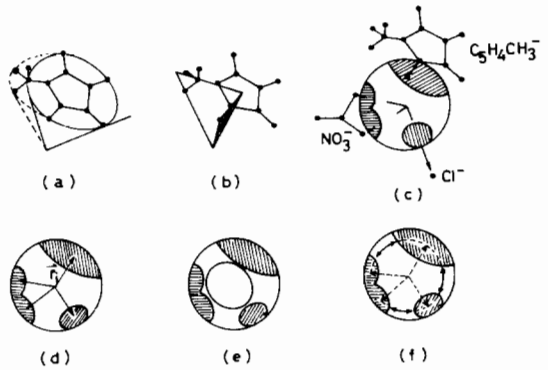

Fig. 2. Unit sphere projection to define the *SAF*, *FA*, $\vec{r}$ of ligands, gaps between them, and holes among them. (a) *SAF*; (b) *FA*; (c) projection of the ligands to a unit sphere; (d) vector $\vec{r}$; (e) hole; (f) gaps.

defined as G = bond angle $(L_1–M–L_2) – (FA_1 + FA_2)$. If two ligand areas are mutually separate, or in contact, or if they overlap, then the gap, G, is positive, zero or negative, respectively.

Besides gap, another symbol, H, is used to describe the hole, referring to the maximum empty cone area between several ligands. Hole is used to express an empty site either for a nucleophilic attack or for activated bonds ready for reactions. It is therefore described also as *SAF* and *FA*. But for a genuine ligand, the ligand border line is defined by the van der Waals sphere of the outmost atom of the ligand, whereas for a hole the border is defined by the maximum sphere circle or sphere ellipsoid between the coordinating ligands.

While Tolman's approach is to study the chemical and physical properties of a complex in relating to the steric parameter of phosphine ligands, our approach in the cone packing model is to study the ligand occupancy in the coordination space and the distribution of the projectional area of ligands on the surface of the unit sphere, and the distortions caused by bonding and steric effect. The dynamic packing model looks into the reaction complex in its transition state by studying relative positions, hard and soft deformations, and the size and shape of the reaction area in the corresponding pathways and reaction products.

Packing Saturation Rule

As mentioned above, the concept of 'coordination saturation' could be interpreted either as saturation of coordination number or as saturation of coordination space. In the case of strong metal–ligand orbital interactions, orbital occupation by electrons is the dominating factor. The formal coordination number in the structures would usually be concen-

trated on electron counting regardless of the space occupation, such as the 18 or 16 electron rules. In actinide organometallic compounds, although favourable electron counting of 20 electrons for uranium and 22 electrons for thorium were noticed [8], they apply only to a limited number of compounds.

If an equilibrium does exist between steric effect and bonding at a certain stage of ligand packing, the energy decrease due to a new ligand coming into the coordination sphere might not be sufficient to compensate for the energy increase caused by the increased non-bonding repulsions. Then the overall packing in the coordination space would be stable at a stage determined by the sum of solid angle factors (*SAS*), while the formal coordination numbers would not necessarily be based on electron counting. Statistics on *SAS* and coordination number distributions would be helpful to distinguish the above two tendencies.

By structural analysis of more than 400 structures of lanthanide and actinide coordination and organometallic compounds, we have found the following:

(a) For a metal ion at a certain oxidation state, fluctuations of *SAS* values are relatively small whereas variations of coordination numbers are great. The total steric packing *SAS* increases slowly with the coordination number, reaching a maximum of 0.90. It is obvious that steric packing prevents the new ligand from coming further into the coordination sphere (Fig. 3).

(b) For the first order approximation, the *SAS* value, which means space efficiency of a metal ion at a certain oxidation state, is relatively stable. For some structures with bulky ligands, the steric crowding may be rather low in the first order, but the second order steric packing in the structure is saturated.

(c) *SAS* increases with increasing oxidation state of the central ion, because in the higher oxidation state the ligand–metal bond strengths have increased. The statistics of the calculations are shown in Table I.

These were referred to as the 'packing saturation rule' or the so-called solid angle sum rule [19]. Saturation packing is not necessarily the closest packing. Saturation packing is reached whenever the hole between the ligands is not big enough to accommodate another, even the smallest, ligand.

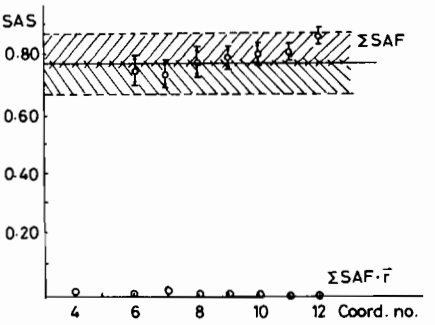

Fig. 3. Packing saturation rule and packing centre rule for lanthanide coordination compounds.

Structures of lanthanides and actinides are stable only when they are packed to saturation. For a compound of supposed structure $MA_nB_mC_p$, steric packing can be calculated by the following equation

$$SAS = nSAF_A + mSAF_B + pSAF_C + \Delta \quad (1)$$

where A, B, C, are the different ligands; and n, m, p and SAF_A, SAF_B, SAF_C are the numbers and the solid angle factors of the ligands, respectively. Δ is the correction of the ionic radii for different lanthanides and actinides.

Steric packing of multi-ligand compounds can be studied in detail using so-called packing diagrams. Normally, the stable region in the diagram is defined with a central line at the average *SAS* of the metal ion concerned, and a deviation of ±0.10, which is the *SAF* value of an ordinary ligand like water, as the borderline. On gain or loss of one ligand, the compound becomes critically unstable due to over- or under-steric crowding. For example, the structure of the ion around uranium(IV) is neither the simple one shown as **A** nor the eight-coordinated complex anion shown as **B**. It is actually either in the form of six-coordinated complex anion C or the eight-coordinated bridged complex **D**.

Even in the stable region, the stability of a supposed structure is dependent on the second order steric crowding. As a principle, ligands of lower second order steric effect, such as Cl^- and NCS^-, tend to form compounds with *SAS* above the average, whereas the bulky ligands tend to form compounds with *SAS* below the average. A few ligands which are very bulky in the second order, like $N(SiMe_3)_2^-$,

TABLE I. Steric Packing of f-Block Coordination and Organometallic Compounds

Metal ion	UO_2^{2+}	U(IV) [3]	Th(IV)	$Ln(III)_{coord}$ [7]	$Ln(III)_{organomet}$ [19]
Structures taken into statistics	80	50	40	140	40
SAS	0.90	0.81	0.81	0.78	0.73
Standard deviation	0.05	0.04	0.05	0.05	0.05

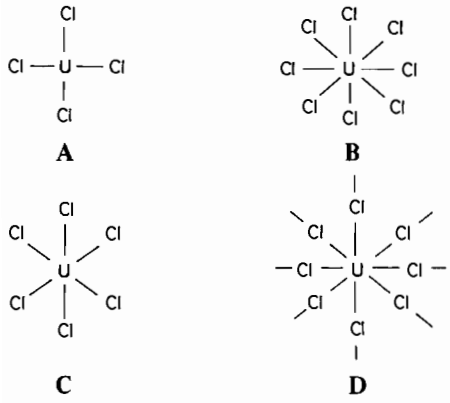

and CMe_3^-, form complexes with *SAS* even below the stable region. The most useful packing diagrams are shown in Fig. 4(a), (b), (c), (d) and (e). In Fig. 4(a) formal coordination number is shown on the abscissa, while the overall steric crowding is represented on the ordinate. The coordination number and *SAS* increase respectively according to eqn. 1.

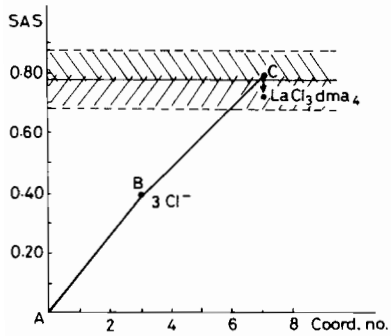

Fig. 4a. Steric packing and coordination number of lanthanide coordination compounds.

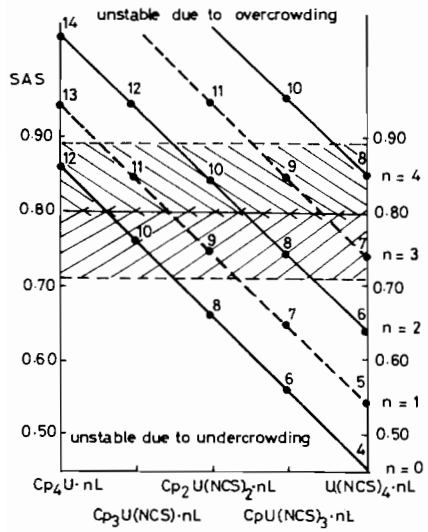

Fig. 4b. Steric packing in uranium(IV) Cp–NCS-neutral ligand ternary system.

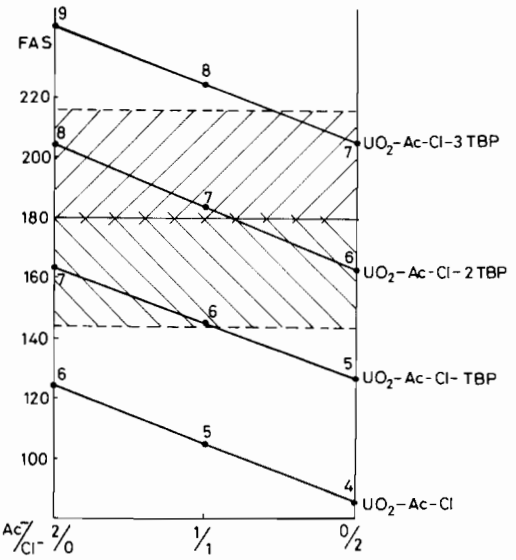

Fig. 4c. Prediction of synergistic extraction of uranyl on acetate–chloride–TBP ternary system.

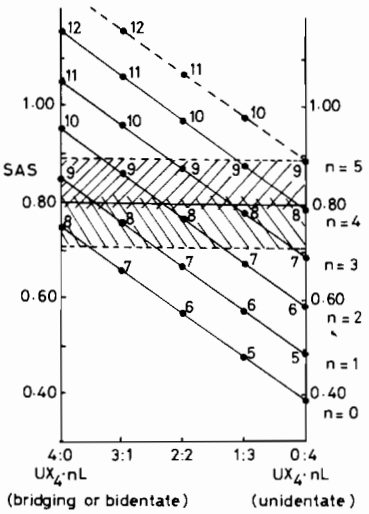

Fig. 4d. Steric packing and possibility of bonding for uranium(IV) halogenoacetate complexes.

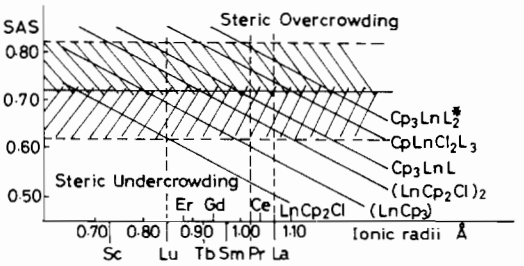

Fig. 4e. Steric crowding of the lanthanide cyclopentadienyl complexes; the new pattern $LnCp_3L_2$ was predicted [6b].

Complexes composed of the same ligands are represented by a straight line while those composed of various ligands are represented by a folded line segment. Thus steric packing of compound $LaCl_3$-dma_4 is represented by AB–BC; the first segment AB represents the three chlorines and the second segment BC represents the steric packing of the four dma ligands. A correction of −0.06 in packing must be included because of the larger lanthanium ions. Another packing diagram is shown in Fig. 4(b), which has so far been used to study mixed-ligand systems. The ratio of the mixed anions is represented on the horizontal line, whereas the overall steric packing is shown on the vertical line. With increasing number of neutral ligands L, steric packing rises step by step. Each point represents a structural pattern denoted by its coordination number and the *SAS* value. We have for the first time used such a graph to explain the stability of the compounds $UCp(NCS)_3L_2$ (Fig. 4(b)). On the two extreme sides are the binary complexes UCp_4L_n and $U(NCS)_4L_n$. It is clearly seen that for proper packing the number of neutral ligands should be zero for the former and three or four for the latter. Based on this expectation, we have prepared the first uranium(IV) thiocyanate complexes with coordination number 7 and determined their structures [9].

Synergistic extraction has so far been studied only in the mixed extractant system,

$$\text{substrate} + \text{extractant}_1 + \text{extractant}_2$$

We hold that the following mixed substrate system might also be applicable for synergistic extraction:

$$\text{substrate}_1 + \text{substrate}_2 + \text{extractant}$$

Based on the expectation that $UO_2AcClTBP_2$ is more properly packed (Fig. 4(c)) than $UO_2Ac_2TBP_2$ and $UO_2Cl_2TBP_2$ and that it might be more stable in the organic phase, we have found a synergistic effect in the extraction of uranyl in mixed extraction substrates of ammonium chloride and sodium acetate [10].

Chelating ligands have different *SAF* values when they are mono- or multidentate because they occupy a different number of coordination sites on different modes of binding. Binding of halogenoacetate in uranium complexes is described in Fig. 4(d). The *SAF* of monodentate halogenoacetate is 0.10 while the *SAF* of the bidentate one is 0.19. The ratio of bidentate to monodentate modes is shown on the abscissa. The greater the number of neutral ligands the complex has, the fewer coordination sites the halogen–acetates hold, and the more favourable it is to the monodentate binding, in consideration of the packing saturation rule and the charge balance [11].

A systematic analysis of the stability trend for lanthanide and actinide compounds of the same pattern can be evaluated in packing diagrams like Fig. 4(e), in which ionic radii are described on the abscissa and the *SAS* value of each structural pattern is described on the ordinate. The overall steric packing decreases linearly with increasing ionic radii [3a]. Each oblique line represents a structure pattern. A new structural pattern of lanthanide organometallic compounds $LnCp_3L_2$ was predicted by drawing such an diagram, and this new pattern was confirmed [6b].

Uniform Packing and Simulation of Molecular Structures

Two extremes can be imagined when studying molecular structures with the unit sphere projection method. On one extreme, the ligand coordination vector and their sum will remain independent of the ligand geometrical factors if the structures are completely determined by the orbital interactions. On the other extreme, molecular structures of ideal ionic compounds are completely determined by the ligand size and shape, because the interactions are like those of charged particles which are non-directional and non-saturated. The actual structures should be intermediate in between these two extremes. From the treatment of more than 150 structures of lanthanide coordination compounds, we have found that the sums of ligand coordination vectors $\vec{r}$, each multiplied by a weighting factor of its *SAF*, *i.e.* $\Sigma SAF \cdot \vec{r}$, always approaches zero. The average value of $\Sigma_{i=1}^{n} SAF_i \cdot \vec{r}_i$ based on statistics for the 150 lanthanide structures is 0.02, with a standard deviation of 0.015. However, the simple sums of the coordination vectors of these compounds are rather scattered. The packing centre rule could be so understood that if a box is filled up with balls, its weight centre should approximately coincide with the box centre.

Molecules of coordination compounds can be regarded as polyhedrons intra-connected with springs (Fig. 1). To have a stable structure, the ligands must be in balanced positions where the stress, both local and overall, is in equilibrium with bonding. The 'uniform packing' actually refers to a stable distribution of charged ligands which arrange themselves according to their size and shape. The packing centre rule is rigorously valid only at infinite coordination number on the metal ion, and with infinitely small ligands. Nevertheless, we hold that the rule is approximately true for a limited number of ligands. Uniform packing is actually a state of packing at the lowest potential energy due to ligand non-bonding repulsions. If the vector $SAF_i \cdot \vec{r}_i$ is taken as the 'packing dipole', then the fact that their sum approaches zero simply implies that the 'packing centre' coincides with the metal ion. If these two

TABLE II. Molecular Geometry of Coordination Pattern MA_3B

Compound	Ligand *SAF*	Reported bond angle (°)		Calculated bond angle (°)
UCp_3Cl	Cp: 0.21 Cl: 0.14 F: 0.093 C: 0.136 (alkyl) [3]	101 116.7	[12]	102.8 115.2
UCp_3F		100 117	[13]	98.5 117.9
$UCp_3C_8H_9$		99.7 117.3	[14]	102.5 115.5
$UCp_3(nBu)$		100.6 116.7	[15]	102.5 115.5
$LaCp_3thf$	Cp: 0.215 thf: 0.087 [6a]	99.5 117.7	[16]	97.8 118.2
$PrCp_3thf$		99.0 117.6	[17]	
$NdCp_3thf$		100.2 117.0	[17]	
$GdCp_3thf$		99.2 117.5	[18]	
YCp_3thf		99.1 117.4	[16]	

centres do not coincide, the molecular structure will distort further until this rule is obeyed. Using this rule we have calculated the molecular structure of lanthanide and actinide organometallic compounds of the pattern MA_3B and found the calculated bond angles are in surprisingly good agreement with the experimental results (Table II).

It is not possible to define a structure by the packing centre rule alone. For example, molecule MA_2B_2 might be either a square planar or a distorted tetrahedron. In both structures $\Sigma_{i=1}^{n} SAF_i \cdot \vec{r}_i = 0$. The term 'uniform' should be further clarified [6c].

In a structure where the 'saturation packing' is reached, the gap angles between ligands are normally very small, usually less than 10°. With the assumption of continuous potential energy function, the potential energy due to the interaction of the neighbouring ligands i, j can be expanded in the Taylor's series (eqn. 1).

$$U_{ij} = U_0 + (\partial U/\partial X)_0 \Delta X + \frac{1}{2}(\partial^2 U/\partial X^2)(\Delta X^2) + \ldots \tag{2}$$

Here ΔX is the gap between ligands and it is proportional to gap angle G_{ij}. The first term U_0 in eqn. 2 is a negative constant, and the second term equals zero because the expansion is at the minimum position. So the changing part of U_{ij} varies as a square of G_{ij}. Close to the equilibrium positions the potential form should be similar to the potential of a spring. So in Fig. 1 the steric interaction is represented by springs connecting the neighbouring ligands.

We have designed the CONPACKS computer program to simulate molecular structures. The computer, on input of either the fan angles or the solid angle factors of the ligand cones, will arrange each cone to a definite position according to the principle $\Sigma SAF \cdot \vec{r} = 0$, and ΣG^2 minimum. By this route, not only could we simulate individual structures, but it was also possible to study steric effects in a systematic way.

The pattern MA_2B_2 is taken as an example (see Fig. 5) with $M = Ln^{3+}$ or An^{4+} and $A = Cp^-$. The bond angles are given on the ordinate and the fan angle of ligand B is given on the abscissa. The bond angle between the two ligands A decreases while the bond angle between two ligands B increases. Bond angle A–M–B increases first, reaching the maximum when $FA_A = FA_B$; at this point the structure becomes a normal tetrahedron. Bond angle A–M–B will decrease with further increase in the size of ligand B.

A diagram to show the five ligand packings is given in Fig. 6, with the supposed compound '$U(C_5H_5)_2Cl_2L$' as an example. It is clearly seen that no matter how large the fan angle of ligand L is, the bond angles Cp–U–Cp and Cp–U–Cl are larger than their fan angles sums, and bond angles Cl–U–L and Cl–U–Cl are always less than the 'fan angle

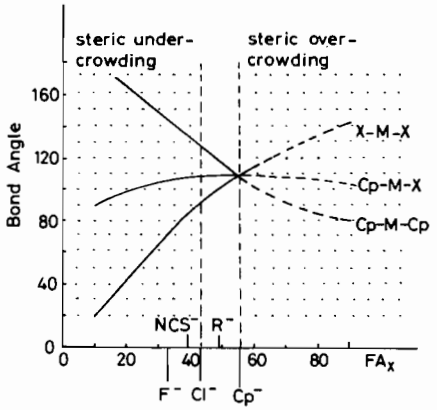

Fig. 5. Molecular geometry of the structural pattern $An(C_5H_5)_2X_2$.

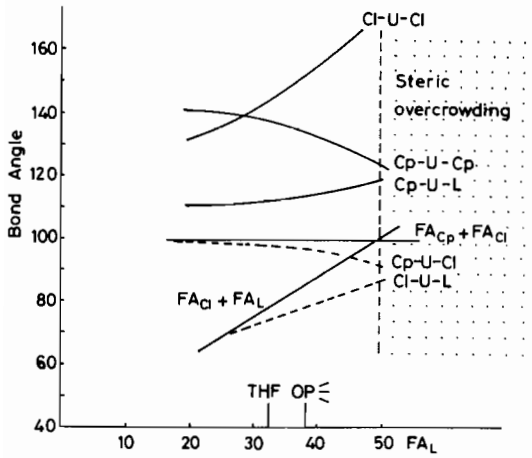

Fig. 6. Molecular geometry of the structural pattern UCp_2Cl_2L.

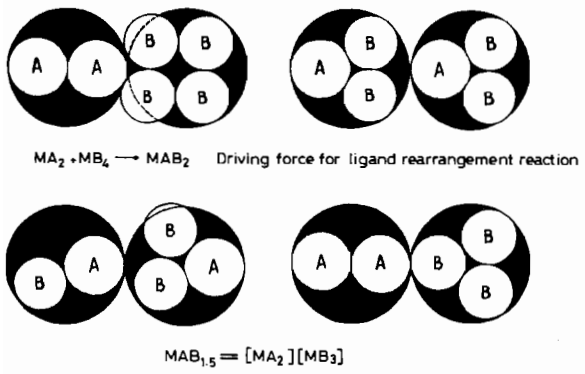

Fig. 7. Rearrangement of the blocks.

sums' of the corresponding ligands $FA_{Cl} + FA_L$ and $FA_{Cp} + FA_{Cl}$. These two pairs of ligands were compressed very tightly and the gaps between them were negative. Instability is caused due to improper packing of this kind. Such a phenomenon is not uncommon in structures with odd number ligand packing in which one local part has very high steric tension while the other part has very loose steric packing. The driving force for the disproportionation might

$$Cp_2UCl_2L \longrightarrow Cp_3UCl + CpUCl_3L_2$$

be the improper packing of Cp_2UCl_2L. This reaction is just like an exchange when playing with toy building blocks (Fig. 7).

Dynamic Packing

If the importance of steric packing in stable structures is acknowledged, there should be no difficulty in understanding that in the reaction process when the bonds are at the instant of forming and breaking, steric effect plays a more profound role than it does in stable compounds.

Most of the organometallic reactions take place at the metal coordination sphere. Although the rules of saturation packing and uniform packing are not obeyed in the reaction process, it is still interesting to simulate the ligand positions, the active area and other properties as a study of 'the excited states of steric packing'. Comparatively, the stable structure is the 'ground state of steric packing'. At the instant of bond formation and breaking, only one or two bonds are changing, whereas most of the bonds in the molecule stay inert. The whole coordination sphere may be divided into the inert sphere and the activated area. The key point is: the border of the active area is defined by the inert area, which could be quantitatively studied by the dynamic cone packing model. The purpose of our work in dynamic packing is to understand:

(1) Geometrical conditions, *i.e.*, quantitative descriptions of the active area needed for reaction intermediates.

(2) Whether the above conditions are satisfied in the actual reaction in the supposed reaction pathways.

(3) Relations between the active area and the reaction products.

We have made a few general assumptions:

(1) For the inert ligands, bond lengths remain unchanged during the reaction process, *i.e.*, $SAF_{dynamic} = SAF_{static}$ for inert ligands.

(2) Inert ligands are hard, almost uncompressible. This means that the gaps between ligand areas could be positive, zero or negative. But when negative, they cannot reach very high, due to the steep increase in the ligand repulsions.

(3) As long as condition 2 is held, the energy barrier for the ligand drift in the coordination sphere is relatively low in comparison to bond breaking between the metal and the ligands.

A reaction undergoes many intermediate states to reach completion. As long as one intermediate is

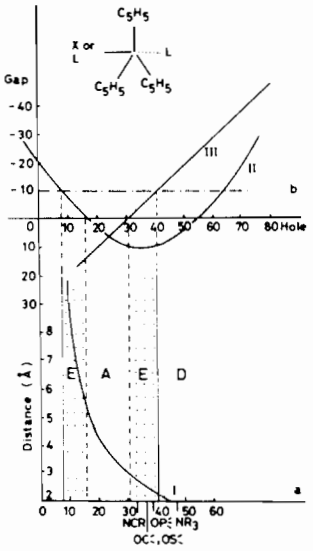

Fig. 8. Lewis base association and dissociation.

prohibited by geometrical conditions, the reaction must go in other directions. By simulating the ligand positions, the area and shape of stable region can be defined. The kinetic accessibility for a special reaction can be predicted. As an illustration, the following examples are given.

(1) Lewis Base Association and Dissociation

In consideration of the following reaction,

$$MCp_3XL \rightleftharpoons MCp_3X + L$$

M = U(IV), X = Cl^-, NCS^-, L = CH_3CN or M = La, Ce, Pr-(III), X = L = CH_3CN, C_2H_5CN

Changes of the gaps between ligands when the free Lewis base is approaching the metal ion in the *trans*-direction to the X group are shown in Fig. 8. The closer the Lewis base comes to the metal ion, the greater the empty space it needs. The other ligands were compressed to be closer to each other. An empty site with a fan angle of at least 30° is needed for the smallest base like CH_3CN to reach the coordination sphere and to form a new bond. At this stage the cyclopentadienyls and the group X (here X refers to the thiocyanate group for quantitative description) begin to contact each other.

As long as one of the gaps becomes negative, potential energy due to ligand–ligand repulsion will increase, which will counteract the energy decrease due to formation of a new bond. Some bulky ligands need more coordination space to form a stable bond; for example, triphenylphosphine oxide, will compress the cyclopentadienyls and the thiocyanate to overlap considerably (gap = −10°) to form a stable bond in the assumed structures, '$Cp_3X(OPPh_3)_2$'. Such an overlap is not allowed because of the high potential energy rising from ligand repulsion; therefore, the above equilibrium shifts only to the right (dissociation) in spite of its high basicity, in contrast to acetonitrile which could shift the equilibrium to the left.

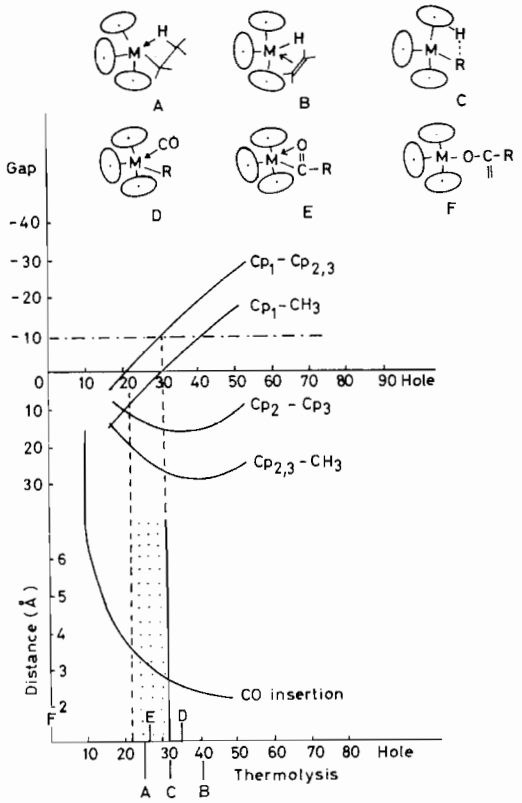

Fig. 9. Thermolysis and CO insertion of metal carbon bond.

2. Thermolysis and Carbon Monoxide Insertion of Metal Carbon σ-Bond

One of the most important modes of metal carbon σ-bond thermolysis is via β-elimination. However, this does not happen in the thermal decomposition of Cp_3UR. Two transition states **A** and **B** are essential for the β-elimination route. It needs a rather large reaction area, in fan angles of about 83° × 33°, to establish transition state **B**. This means that the other ligands have to be compressed into highly negative overlappings (see Fig. 9); this requires a very high activation energy and thus is inaccessible in thermolysis but possible in photolysis.

An interesting point is that in the process of transition from state **A** to state **B**, the alkyl group will unavoidably be compressed into contact with the cyclopentadienyls. Hydrogen abstraction from cyclopentadienyl to the alkyl group then occurs. It is clearly seen that the geometrical condition for the ring hydrogen abstraction (transition state **C**) is $G_{Cp-R} = 0$, which is reached ahead of transition state **B**. We hold that this is the reason that Cp_3UR decomposes via the ring abstraction route.

Similar analysis is made for carbon monoxide insertion into the metal-carbon bond. A series of transition states **D**, **E**, **F** were geometrically simulated and indicated in Fig. 9. There is little problem with energy barriers for the transition states **E** and **F** because they do not need a very large reaction area and hence do not need to compress the cyclopentadienyls too much. The interesting point is: whereas the transition state **E** is quite properly packed and could stay as a stable structure, the end product **F** will dimerize in various ways because of its understeric crowding.

Conclusion

The cone packing model describes the molecular structures of coordination compounds as ligand cones joined at the same apex. Many classical concepts such as coordination saturation, molecular geometry, reaction pathways, ligand rearrangement and disproportionation (Fig. 7), as well as other problems which are not discussed in the present paper such as the irregular bond lengths in many lanthanide and actinide structures, can be explained with this simple model. In conclusion, steric effect due to geometrical factors is quite important, and it deserves more attention in quantitative study.

Acknowledgements

This work was supported by the Science Fund of the Chinese Academy of Science. We gratefully thank Professor Lu Gia-Xi for his helpful discussion and generous support of this work. We also thank Professor K. W. Bagnall and Professor R. D. Fischer for their encouragement and helpful discussions at an earlier stage of the work.

References

1 (a) C. A. Tolman, *J. Am. Chem. Soc., 92*, 2956 (1970); (b) C. A. Tolman, *Chem. Rev., 77*, 313 (1977).
2 (a) J. D. Smith and J. D. Oliver, *Inorg. Chem., 17*, 2585 (1978); (b) G. Ferguson, P. J. Roberts, E. C. Alyea and M. Khan, *Inorg. Chem., 17*, 2695 (1978).
3 (a) Li Xing-fu, *Ph.D. Qualification Research Report*, University of Manchester, 1980; (b) Li Xing-fu, *Ph.D. Thesis*, University of Manchester, 1982; (c) K. W. Bagnall and Li Xing-fu, *J. Chem. Soc., Dalton Trans.*, 1365 (1982).
4 A. J. Smith, in G. Bombieri, G. de Padi and P. Zanella (eds.), 'Proc. 11èmes Journées des Actinides, Lido de Jesolo, Italy, May 25–27, 1981', CNR, Padua, Italy, 1982, p. 64.
5 (a) S. N. Titova, V. T. Bychkov, G. A. Domrachev, G. A. Razuvaev, L. N. Zakharov, G. G. Alexanohov and Y. T. Struckov, *Inorg. Chim. Acta, 50*, 71 (1981); (b) E. B. Lobkovskii, *Zh. Strukt. Khim., 24*, 66 (1983).
6 (a) Li Xing-fu and R. D. Fischer, *Abstr. First Int. Conf. Chem. Technol. of Lanthanides and Actinides*, Venice, Sept. 5–10, 1983, *Inorg. Chim. Acta, 94*, 50 (1983); (b) Li Xing-fu, S. Eggers, J. Kopf, W. Jahn, R. D. Fischer, C. Apostolidis, B. Kanellakopulos, F. Benetollo, A. Polo and G. Bombieri, *Inorg. Chim. Acta, 100*, 183 (1985); (c) Xu Ying-ting, Li Xing-fu, Feng Xi-zhang, Sun Peng-nian and Shi Jie, *Sci. Sin.*, submitted for publication.
7 (a) Li Xing-fu, Feng Xi-zhang, Xu Ying-ting, Sun Peng-nian and Shi Jie, *Acta Chim. Sin., 43*, 502 (1985); (b) Sun Peng-nian, Shi Jie, Feng Xi-zhang, Xu Ying-ting, Li Xing-fu, Wang Wen-qing and Yi min, *Acta Chim. Sin., 43*, 597 (1985).
8 T. J. Marks, J. M. Manriquez, P. J. Fagan, V. W. Day and S. H. Vollmer, in N. M. Edelstein (ed.), 'Lanthanide and Actinide, Chemistry and Spectroscopy', A.C.S. Symposium Series, No. 131, 1980, p. 3.
9 K. W. Bagnall, Li Xing-fu, G. Bombieri and F. Benetollo, *J. Chem. Soc., Dalton Trans.*, 19 (1982).
10 Li Xing-fu, Shi Jie, Tang Ber-lin, Sun Peng-nian, Wang Hai-tung and Feng Xi-zhang, *Acta Chim. Sin.*, in press.
11 K. W. Bagnall, O. V. Lopez and Li Xing-fu, *J. Chem. Soc., Dalton Trans.*, 1153 (1983).
12 Wang Chi-hsiang, Yen Tung-mou and Lee Tseng-yuh, *Acta Crystallogr., 18*, 340 (1965).
13 R. R. Ryan, R. A. Penneman and B. Kanellakopulos, *J. Am. Chem. Soc., 97*, 4258 (1975).
14 G. Perego, F. Farina and G. Lugli, *Acta Crystallogr., Sect. B, 42*, 3034 (1976).
15 G. W. Halastead, E. C. Baker and K. N. Raymond, *J. Am. Chem. Soc., 97*, 3049 (1975).
16 R. D. Rogers, J. L. Atwood, A. Emad, D. J. Sikara and M. D. Rausch, *J. Organomet. Chem., 216*, 383 (1981).
17 Fan Yuguo, Lü Pinzhe, Jin Zhongsheng and Chen Wenqi, *Sci. Sin., Ser. B, XXVII*, 994 (1984).
18 R. D. Rogers, R. D. Bynum and J. L. Atwood, *J. Organomet. Chem., 192*, 65 (1980).
19 R. D. Fischer and Li Xing-fu, *J. Less-Common Met., 112*, 303 (1985).